Experimental Investigation of Flame Dynamics of Swirled Methane-Air Flame with H_2 addition

S. Bonuso*, P. Di Gloria*, G. Mehdi*, M.G. De Giorgi*
sara.bonuso@unisalento.it
*University of Salento, Lecce, Italy

Abstract

This study investigates the impact of hydrogen enrichment on flame structures while maintaining a constant thermal output of 5.06 kW. High speed chemiluminescence images were captured for two fueling conditions: pure methane/air and methane with hydrogen addition. The results show that hydrogen enrichment leads to a slightly shorter flame length and a wider flame angle due to increased expansion in the Combustion Recirculation Zone. UV emissions are significantly affected, with a shifted luminosity zone and reduced variance. Proper Orthogonal Decomposition (POD) and Singular Proper Orthogonal Decomposition (SPOD) analyses reveal coherent structures and energetic modes. Hydrogen enrichment results in smaller structures near the nozzle exit, longitudinal oscillations, and vortex shedding. The findings enhance our understanding of hydrogen's impact on flame characteristics and contribute to improving flame stability.

Introduction

The gas turbine industry is exploring lean premixed combustion of hydrogen-enriched fuel blends as a promising solution for reducing greenhouse gas emissions and NOx emissions [1]. Many gas turbines currently have the capability to burn mixtures of hydrocarbons and hydrogen in varying proportions [2, 3]. However, efficiently mixing hydrogen and air prior to combustion is challenging, and micromixing technologies have been developed to prevent high-temperature stoichiometric reaction layers at the hydrogen injector outlet, which can lead to high NOx emission levels and thermal stress [4-6]. This study proposes an alternative approach of injecting hydrogen into a conventional swirl burner, enabling partial premixing with methane before combustion to avoid the formation of diffusion reaction layers, without requiring significant combustor redesign [7]. The study then analyzes the effects of H2-enrichment on flame shape and dynamics using modal decomposition techniques. To properly identify, separate, and temporally resolve dynamic components, the study employs spectral proper orthogonal decomposition (SPOD), a modified version of the traditional POD technique that incorporates spectral analysis [8, 9].

Experimental Characterization

In this experimental study, a burner with a square section area of 105 mm width and

360 mm height was used to investigate the swirl flames. The atmospheric nozzle, consisting of two co-rotating swirlers, was used to generate swirl flames inside the burner. More details on the experimental apparatus can be found in Figure 1.

The flowrate of pure methane in the first case and hydrogen and fuel in the second one were calculated to assure that the thermal power remained constant at 5.06 kW. In particular, in the first case, the CH_4 flowrate is equal to 9.33 l/min while in the second one the H_2 flowrate is 3.33 l/min (i.e. the 5% by mass and about the 30% by volume of the total flow rate of mixture) and CH_4 flowrate is 8.32 l/min. The starting equivalence ratio (ϕ value) for ignition was fixed at 0.748, and in the case of the mixture, it slightly decreased to 0.734. The experiments were conducted under constant inlet air flow rate conditions, with a value of 113.3 l/min.

In the present study, high-speed imaging of reaction zone chemiluminescence was utilized to investigate the spatio-temporal distribution of the flame front and primary combustion zone. The emissions were acquired using a Phantom M320S camera equipped with a Lambert image intensifier, as shown in Figure 1. No spectral filtering was applied during imaging. The grayscale images were captured at a framerate of 1000 Hz, with each pixel point being discretized using 8 bits ranging from 0 to 255. Proper Orthogonal Decomposition (POD) and Spectral Proper Orthogonal Decomposition (SPOD) were used in this study to perform modal spatio-temporal characterization of the flame using high-speed acquisitions. [8,9]

Results

High-speed chemiluminescence imaging of reaction zones.

Chemiluminescence images were recorded (without any spectral filtering) for both cases, without and with H_2-enrichment of methane fuel at high-speed (1000 frames/sec framing rate). Such imaging was performed to compare the appearance of reaction zones at the presence of H_2 percentage addition to methane fuel.

The broadband chemiluminescence techniques are utilized to qualitatively examine the impact of hydrogen addition on flame structure. The captured images utilize the same ICCD settings for both the conditions with and without hydrogen at a constant thermal power, facilitating a comparison of the relevant differences.

In Figure 2a, the image in the first column was acquired with pure methane/air, and in the second one with the presence of hydrogen.

Figure 2 provides an analysis of the average flame structures, offering an overall insight into the impact of hydrogen addition on the flame structure. When the fuel mixture is enriched with hydrogen, the mean flame length is slightly shorter compared to case of pure methane, and the flame angle is wider. This phenomenon is attributed to the increased expansion of the burnt gases within the Combustion Recirculation Zone (CRZ) due to the higher rate of heat release. The flame root position however does not differ significantly from the two cases even if the position of the maximum of heat release rate is located closest to the burner exit in the case of H_2 addition. It was noticed that the effects of hydrogen presence on the UV emissions were more significant and it was noted that the luminosity zone was shifted to the nozzle exit. The UV variance was greatly reduced with the use of hydrogen. The reductions of fluctuations lead to improved flame stability. To better understand how hydrogen enhances combustion, the Proper Orthogonal Decomposition (POD) method is employed to identify the coherent structures and energetic modes of the flame.

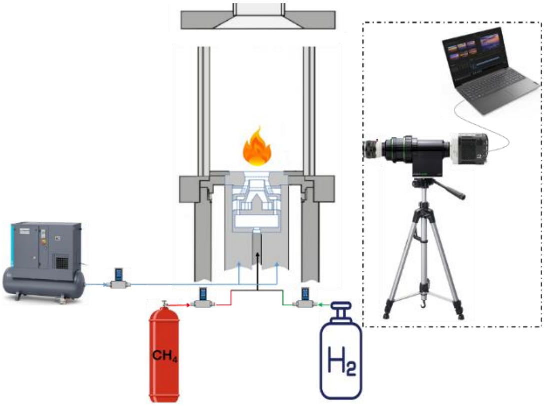

Figure 1 Experimental setup.

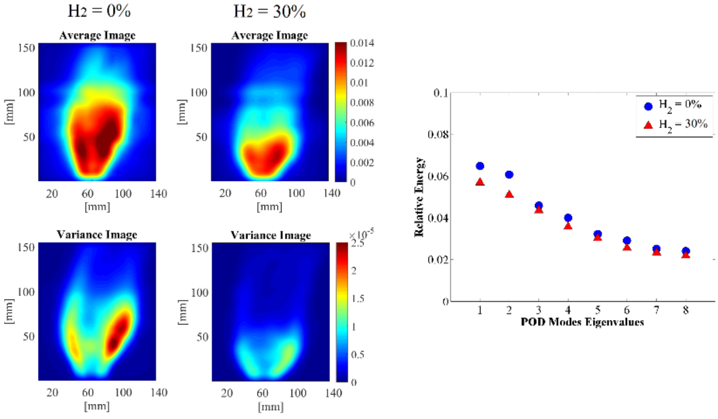

a)

b)

Figure 2. a)Time-averaged and variance of the broadband chemiluminescence signal (line-of-sight) without and with H_2 addition; b) Relative Energy of the details of POD of chemiluminescence images

The POD technique separates dynamic data into orthogonal modes that are arranged by decreasing energy, with the lowest order mode having the most energy. The energy contribution of each mode to the flow field reconstruction is described by their energy. Figure 2b illustrates the relative energy contributions of the 1-8 eigenmodes (fluctuations) with and without the hydrogen addition. It was observed that the first 8 modes generally account for the majority of the relative energy. Additionally, it was noted that the energy content of the first mode in the hydrogen/methane flame was lower than that of the pure methane flame. It is evident that with the use of hydrogen, the heat fluctuations of modes 1-8 were decreased in the first few modes. This decrease in energy content for the mixture flame can be attributed to the stabilizing effect of the hydrogen, which results in lower heat release fluctuations that are represented by the energy content in the highest modes.

In Figure 3, a comparison is presented between the first four POD modes for UV chemiluminescence images in two cases: one without hydrogen addition and another with hydrogen addition. The contour plots illustrating the mode shapes are arbitrary in terms of scale and sign, as they are scaled by their respective time coefficients, the colour red and blue are used to highlight zones with the highest intensity of fluctuations. However, these colours represent opposite changing directions, indicating a phase difference π between different zones. It is important to note that these modes represent the fluctuations in heat, ordered from the most energetic mode (1^{st} mode).

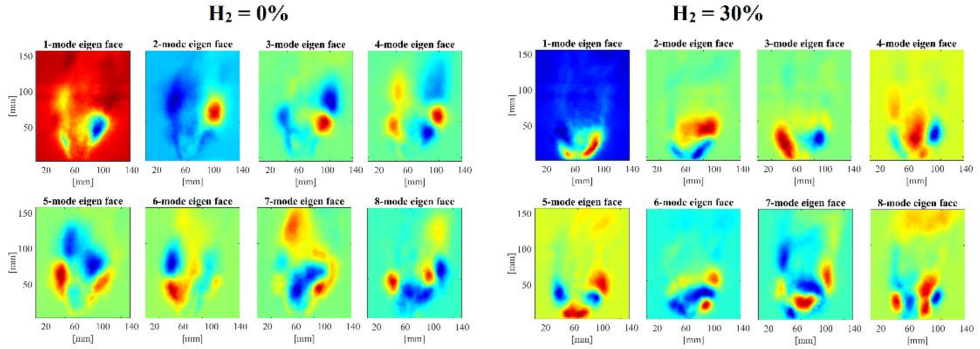

Figure 3. Proper Orthogonal Decomposition of chemiluminescence images.

Higher modes show coherent structures that can be correlated with flow features. As the mode number increases, the wavenumber of this motion increases.

In the methane flame, larger-scale coherent structures that start from the exit of the burner and then develop downstream are evident. In particular, the first two modes display rotating fluctuations, while the third and fourth modes exhibit vortex shedding along the shear layers near the burner exit. Additionally, the fourth mode demonstrates an alternate ring vortex propagation in the swirl combustion mode. The enrichment with H_2 leads to smallest structures closest to the nozzle exit, with an longitudinal oscillation in the second mode, while vortex shedding can be clearly observed in modes 3 and 4.

Frequency analysis of heat and acoustic signals.

In order to gain a better understanding of flame fluctuations, a simultaneous evaluation of the power spectral density (PSD) has been conducted from both microphone signals and the Proper Orthogonal Decomposition (POD) eigenmodes for different cases (Figure 4). The addition of hydrogen to methane had a notable influence on the frequency of fluctuations observed in both the acoustic signal and POD modes, which can be qualitatively linked to heat transfer. Clearly, distinct frequencies emerge as dominant within the combustor when comparing fuels with and without hydrogen. Microphone measurements revealed broadband sound spectra with minor peaks around 124 Hz, 209 Hz, 417 Hz, and 536 Hz for the methane case. These frequencies align with the findings of previous studies [10], particularly the peak at 530 Hz, which was associated with the Precessing Vortex Core (PVC).

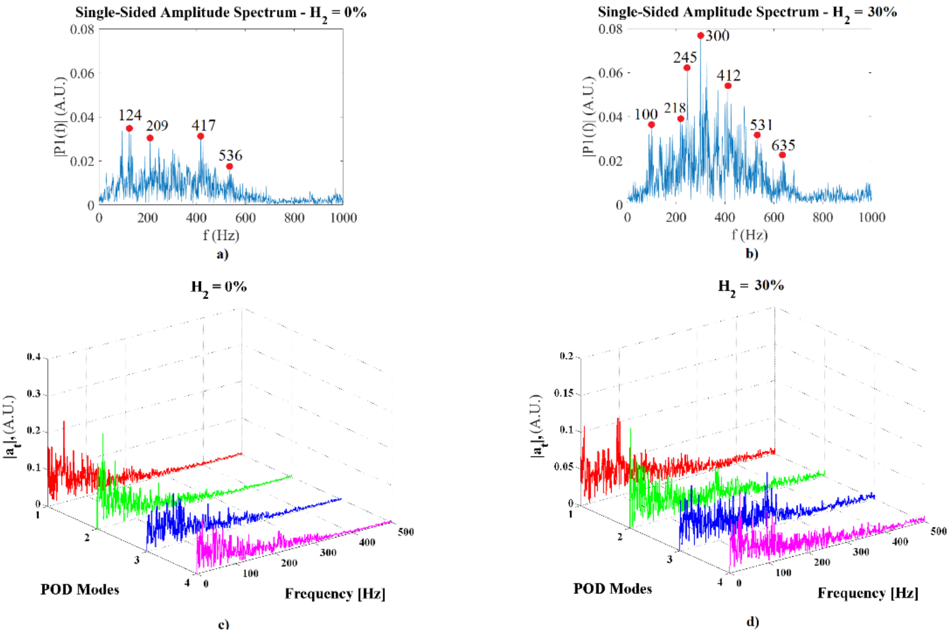

Figure 4. Power spectral density of microphone signal with pure methane (a) and with hydrogen enrichment (b); POD eigenmodes.

In [10], the acoustic peaks observed at higher frequency ranges (greater than 530 Hz) were found to be correlated with the acoustic modes of the combustor. The amplitude of these acoustic mode peaks increased with a higher percentage of hydrogen in the fuel, which was also evident from the audible signature of the reaction zones during experiments. Additionally, in our present study, a certain level of sound power was concentrated in the frequency band close to 635 Hz when hydrogen was added. The introduction of hydrogen resulted in frequencies falling within the same bands (100 Hz, 245 Hz, 412 Hz, and 531 Hz) and other peaks at 300 Hz and 635 Hz, with a significant portion of the sound power concentrated near 300 Hz. Importantly, higher values of peak sound intensity indicate combustion-induced instabilities that could potentially cause damage to the system. However, the high frequencies near 635 Hz were not observed in the PSD of the POD eigenmodes. Combustion-induced instabilities, which can generate large pressure oscillations or sound levels, have the potential to harm the system and should be avoided. Therefore, the benefits of hydrogen addition in terms of emissions must be carefully considered in relation to the requirement of ensuring the structural integrity of the combustor.

Regarding the POD eigenmodes, the peaks are within the frequency range of 0-220 Hz. Specifically, for pure methane flames, high peaks were observed in the range of 0-100 Hz for the first two modes, which are characterized by rotating and transversal oscillations. In modes 3 and 4, there was evident content around 200 Hz, indicating longitudinal oscillations. In the case of hydrogen addition, longitudinal oscillations were present from the second mode onwards, leading to an increase in content around 218 Hz. This frequency was also noticeable in the microphone signal. The first mode exhibited a peak at 93 Hz, close to the 100 Hz peak detected in the microphone measurements.

Spectral Proper Orthogonal Decomposition.

The SPOD analysis of the methane flame, depicted in Figure 5a, highlights a significant energy concentration in the low-frequency range, prominently peaking at approximately 15 Hz. Moreover, a distinct peak is observed around 210 Hz in the high-frequency range. Upon enriching the methane fuel with H_2, there is a reduction in energy intensity within the low-frequency range. Interestingly, a novel peak emerges at approximately 90 Hz. It is noteworthy that despite the H_2 enrichment, the original peaks at 15 Hz and 210 Hz persist. The first SPOD mode at the frequency of about 15 Hz exhibits rotating structures, corresponds to one of the dominant modes that was less clear by the POD analysis. The rotating structures captured in this mode signify the presence of transversal flame oscillation, indicating the whirling nature of the reaction zone. These rotating structures are larger in the case of methane flame. The first mode at a high frequency, approximately 210 Hz, reveals distinct longitudinal oscillations in both fueling conditions. In the case of H_2 enrichment, at a frequency of 93.75 Hz, the first mode exhibits an approximately axisymmetric fluctuation. In this mode, the strong response area alternates between upward and downward directions, indicating vigorous axial movement of the flame within the spatial domain. These characteristics signify an axial oscillation mode, where the flame moves forcefully along the axial direction.

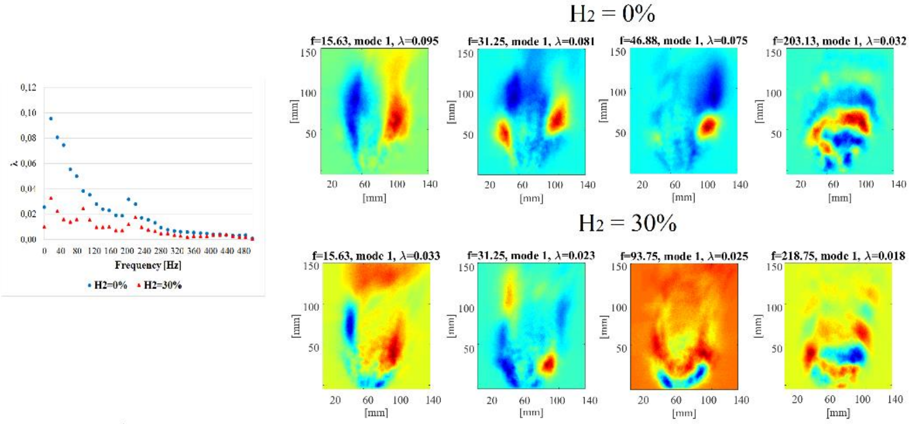

a) b)

Figure 5. SPOD of chemiluminescence images: a) SPOD energy content; b) Mode 1 at selected frequency values.

Conclusions

This study compared chemiluminescence images of flame structures in two fueling conditions: pure methane/air and methane with hydrogen enrichment. The addition of hydrogen resulted in a slightly shorter flame length and wider flame angle due to increased expansion in the Combustion Recirculation Zone. UV emissions were significantly affected, with a shift in the luminosity zone and reduced variance. Proper Orthogonal Decomposition (POD) and Singular Proper Orthogonal Decomposition (SPOD) analyses revealed coherent structures and energetic modes. Hydrogen enrichment led to smaller structures near the nozzle exit, longitudinal oscillations, and vortex shedding. Overall, hydrogen influenced flame characteristics and improved stability. The addition of hydrogen to methane fuel significantly also influenced the frequency of flame fluctuations, both in the acoustic signal and the POD modes.

Reference

[1] Chiesa P, Lozza G, Mazzocchi L. Using hydrogen as gas turbine fuel. J Eng Gas Turbines Power 2005;127(1):73e80. https://doi.org/10.1115/1.1787513.

[2] Lam K-K, Geipel P, Larfeldt J. Hydrogen enriched combustion testing of Siemens industrial SGT-400 at atmospheric conditions. J Eng Gas Turbines Power 2015; 137 (2):21502. https://doi.org/10.1115/1.4028209

[3] Bothien MR, Ciani A, Wood JP, Fruechtel G. Toward decarbonized power generation with gas turbines by using sequential combustion for burning hydrogen. J Eng Gas Turbines Power 2019; 141(12):121013. https://doi.org/10.1115/1.4045256

[4] Dahl G, Suttrop F. Engine control and low-NOx combustion for hydrogen fuelled aircraft gas turbines. Int J Hydrogen Energy 1998;23(8):695e704. https://doi.org/10.1016/S0360-3199(97)00115-8.

[5] Cozzi F, Coghe A. Behavior of hydrogen-enriched nonpremixed swirled natural gas flames. Int J Hydrogen Energy 2006;31(6):669e77. https://doi.org/10.1016/j.ijhydene.2005.05.013.

[6] Oh J, Hwang J, Yoon Y. EINOx scaling in a non-premixed turbulent hydrogen jet with swirled coaxial air. Int J Hydrogen Energy 2010;35(16):8715e22. https://doi.org/10.1016/j.ijhydene.2010.04.159.

[7] Funke HH-W, Beckman N, Keinz J, Horikawa A. 30 years of dry-low-NOx Micromix combustor research for hydrogenrich fuels: an overview of past and present activities. J Eng Gas Turbines Power 2021;143(7):71002. https://doi.org/ 10.1115/1.4049764.

[8] Lumley, J. L. 1967. The structure of inhomogeneous turbulence. Atmospheric Turbulence and Wave Propagation. AM Yaglom, VI Tatarski, 166-178.

[9] Sirovich, l. 1987. Turbulence and the dynamics of coherent structures part iii: dynamics and scaling. Quarterly of Applied Mathematics, 45(3): 583-590.

[10] Rishi Roy, Ashwani K. Gupta, Performance enhancement of swirl-assisted distributed combustion with hydrogen-enriched methane, Applied Energy, Volume 338, 2023, 120919, ISSN 0306-2619, https://doi.org/10.1016/j.apenergy.2023.120919.